Available online at www.sciencedirect.com
SCIENCE DIRECT®
ELSEVIER
International Journal of Impact Engineering 31 (2005) 825–841
INTERNATIONAL JOURNAL OF IMPACT ENGINEERING
www.elsevier.com/locate/ijimpeng

Resistance of high-strength concrete to projectile impact

M.H. Zhang[a,*], V.P.W. Shim[b], G. Lu[a], C.W. Chew[a]

[a] *Department of Civil Engineering, National University of Singapore, 1 Engineering Drive 2, Singapore 117576, Singapore*
[b] *Department of Mechanical Engineering, National University of Singapore, Singapore*

Received 17 November 2003; received in revised form 5 April 2004; accepted 6 April 2004

Available online 11 June 2004

Abstract

This paper presents the results of an experimental study on the impact resistance of concrete with compressive strengths of 45–235 MPa when subjected to impact by 12.6 mm ogive-nosed projectile at velocities ranging from ~620 to 700 m/s. The results indicate that the penetration depth and crater diameter in target specimens exhibit an overall reduction with an increase in the compressive strength of the concrete. However, the trend is not linear. Further increase in the compressive strength requires a reduction in the water-to-cementitious material ratio and the elimination of coarse aggregates. However, doing these does not result in reduction of the penetration depth and crater diameter. The presence of coarse granite aggregates appears to be beneficial in terms of reducing penetration depth, crater diameter, and crack propagation, thus contributing to impact resistance. Incorporation of steel fibers in the concrete reduced the crater diameter and crack propagation, but did not have a significant effect on penetration depth. An increase in the curing temperature from 30°C to 250°C did not alter the impact resistance of the concrete significantly. Based on the present findings and cost consideration, high-strength fiber-reinforced concrete with a compressive strength of ~100 MPa appears to be most efficient in protection against projectile impact.

Keywords: Concrete; Crater diameter; Fiber; High-strength; Penetration depth; Projectile impact

1. Introduction

Concrete structures subjected to impact by projectiles or shell fragments exhibit responses that differ from those when they are under static loading. Projectiles or fragments generate localized

*Corresponding author. Tel.: +65-874-2273; fax: +65-779-1635.
E-mail address: cvezmh@nus.edu.sg (M.H. Zhang).

0734-743X/$ - see front matter © 2004 Elsevier Ltd. All rights reserved.
doi:10.1016/j.ijimpeng.2004.04.009

Nomenclature

C_3A	calcium aluminate ($3CaO \cdot Al_2O_3$)
CRH	caliber radius head
w/c	water-to-cement ratio
w/cm	water-to-cementitious material ratio

effects characterized by penetration or perforation, spalling and/or scabbing, as well as more widespread crack propagation. The magnitude of damage depends on a variety of factors such as impact velocity, the mass, geometry and material properties of the projectile or fragment, as well as the material properties and reinforcement of the concrete target structures.

This paper presents results from an experimental study on the impact resistance of concrete with compressive strengths of 45–235 MPa impacted by 12.6 mm ogive-nosed projectile at velocities ranging from ~620 to 700 m/s. The effects of the compressive and flexural tensile strength of the concrete, the presence of coarse aggregate or steel fibers, and the curing temperature of the concrete are discussed. (In this study, composites without coarse aggregate are also referred to as concrete for simplicity.)

2. A review of impact resistance of high-strength concrete

Resistance to penetration and perforation of plain and reinforced concrete by non-deformable projectiles has been studied long before the technology of high-strength concrete was developed. Most of the work published so far has been based on concrete with compressive strengths of up to ~200 MPa.

In a review on penetration resistance of concrete by Clifton [1], it was reported that some studies showed that the volume of the crater produced when concrete is subjected to impact or impulsive loading, varies approximately inversely with the square root of the compressive strength of concrete. However, other works referenced by him did not show any correlation between compressive strength and impact resistance.

Results from perforation experiments by Hanchak et al. [2] on concrete with compressive strengths of 48 and 140 MPa showed that at lower impact velocities of ~300 m/s, the concrete targets ($610 \times 610 \times 178$ mm) with a compressive strength of 48 MPa were perforated, whereas similar sized targets with a strength of 140 MPa were not. However, for impact velocities between 300 and 1100 m/s, a three-fold increase in unconfined compressive strength resulted in relatively minor improvement of the perforation performance, based on the residual velocity of the projectiles. It was postulated that penetration resistance in the crater region was not sensitive to compressive strength.

In another experimental study by Dancygier and Yankelevsky [3] on the response of concrete to hard projectile impact, it was observed that the projectile penetration depth in concrete with a compressive strength of ~100 MPa was smaller than that in concrete with a strength of ~35 MPa. This showed that a higher compressive strength enhances

resistance against dynamic punching, although it also increased target brittleness and the crater diameter in the event of failure. They observed a reduced brittleness when steel fibers were incorporated into high strength concrete. A comparison of crater dimensions in fiber-reinforced and plain concrete specimens shows that the fibers tend to arrest cracks and thus minimize the damage area.

For concrete with steel fiber reinforcement of up to $\sim$3% by volume, the experimental results of Anderson et al. [4] for tests on fiber-reinforced concrete targets subjected to high velocity projectile impacts indicate that the penetration resistance of concrete, measured in terms of penetration depth, is not greatly influenced by fiber type and content. However, their results showed that a larger fiber content leads to smaller crater volumes.

A study of high velocity projectile impact on slurry infiltrated fiber concrete (SIFCON) by Anderson et al. [5] confirmed the effectiveness of fibers in reducing damage via spalling and scabbing. It was also observed that the gravel in concrete was effective in preventing perforation of specimens. Hence, it was suggested that a composite with both gravel and fibers might provide an optimum solution to reduce overall damage.

From an experimental study on the impact resistance of high-strength concrete, O'Neil et al. [6] found that the penetration depth induced by 0.9 kg projectiles in high-strength concrete with a compressive strength of 157 MPa was approximately 50% less than that in concrete with a compressive strength of 35 MPa, and about 30% less than that in concrete with a strength of 104 MPa. They also found that the incorporation of fibers does not significantly reduce penetration depth, but it does reduce visible damage.

In a research effort by Langberg and Markeset [7] on concrete with compressive strengths of 30–200 MPa, it was found that the penetration resistance of high strength concrete was significantly better than normal strength concrete. However, increasing the cylinder strength of concrete beyond 150 MPa did not provide significant improvement in penetration resistance. After considering the production cost in relation to the penetration resistance for concrete of different strengths, they concluded that for a given level of protection, concrete with a compressive strength of $\sim$90 MPa had the lowest cost.

3. Principles and development of high strength concrete

Concrete is a composite material with coarse and fine aggregates embedded in cement paste matrix. Hence, its mechanical behavior is influenced by the aggregate and cement paste, as well as the interfacial zone between them. In ordinary concrete, the aggregate is the strongest component, whereas the interfacial zone is typically the weakest link due to its higher porosity and higher concentration of large $Ca(OH)_2$ crystals relative to those in the cement paste. Also, the difference in the modulus of elasticity between the aggregate and the cement paste causes stress concentrations between these two components when concrete is subjected to load. In general, the larger the aggregate particles, the greater the stress concentration is. Therefore, cracks and failure planes typically go through the interfacial zone when ordinary concrete is subjected to static loading.

In order to increase the compressive strength of concrete, it is essential to increase the strength of the cement paste and improve the interfacial zone, thus reducing the potential stress

concentration between the aggregate and the cement paste. The former can be achieved by reducing the water-to-cement ratio (w/c), using fine pozzolanic materials such as silica fume, or a combination of these. The latter can be achieved by reducing the maximum aggregate size. For high strength concrete, the strength of the cement paste and the interfacial zone can be improved substantially by the reduction in the w/c ratio and the use of silica fume; consequently, the aggregates often then become the weakest link. Therefore, the use of strong aggregates is essential.

Based on current knowledge, concrete with a 28-day compressive strength of 100 MPa can be achieved easily both in laboratories and at worksites by the use of appropriate aggregates. With stronger aggregates, compressive strengths of 150 MPa can be achieved using conventional production techniques. Reactive powder concrete with compressive strengths of up to ~800 MPa and good toughness has been fabricated under high temperatures of 400°C and pressures of 50 MPa, as reported by Richard and Cheyrezy [8]. Other cementitious composites with high strength and good toughness developed so far include SIFCON [9], slurry infiltrated mat concrete (SIMCON) [10], and ductile concrete (DUCON) [11].

4. Experimentation

4.1. Mix proportions of concrete and preparation of specimens

In order to evaluate the impact resistance of concrete of different compressive strengths, 11 concrete mixtures were formulated and their mix proportions are given in Table 1. Concrete mixtures NC 40 and NC 60 contained coarse aggregate with a maximum nominal size of 20 mm. Concrete mixtures NC 90 and NC 120 contained coarse aggregate with a maximum size of 10 mm.

Table 1
Mix proportions of concrete

Mix ID	w/cm	Cement (kg/m^3)	Silica fume (kg/m^3)	Water (kg/m^3)	Coarse aggregate (kg/m^3)	Natural sand (kg/m^3)	Quartz sand (kg/m^3)	Steel fibers (kg/m^3)	Admixture (kg/m^3)
NC40		360	—	198	1105	737	—	—	—
NC60	0.45	440	—	198	1090	666	—	—	—
NC90	0.31	475	—	143	1064	709	—	—	10[a]
NCF90	0.31	468	—	141	1048	698	—	118	10[a]
NC120	0.27	475	48	133	952	779	—	—	15[a]
NCF120	0.27	468	47	131	938	767	—	118	15[a]
CM	0.23	714	179	188	—	—	1320	—	18[b]
QFF	0.23	704	176	185	—	—	1300	119	18[b]
QWF	0.23	704	176	185	—	—	1300	119	18[b]
QOF-1	0.23	704	176	185	—	—	1300	119	18[b]
QOF-2	0.18	707	177	145	—	—	1365	119	18[b]

[a] Retarding admixture.
[b] Superplasticizer.

To reduce the heterogeneity of the concrete and to increase its compressive strength, no coarse aggregate was used for the remaining concrete mixtures.

The water-to-cementitious material ratio (w/cm) of the concrete ranged from 0.18 to 0.55 and the corresponding compressive strength ranged from 237 to 45.5 MPa. Some of the mixtures contained 1.5% steel fiber by volume in order to improve toughness and impact resistance.

All specimens subjected to impact tests had a common size of 300×170 mm and a thickness of 150 mm. As the specimens were relatively thick, neither perforation nor damage in the form of scabbing at their distal face was observed. For most of the mixtures, three specimens were subjected to the impact tests. Three cubes were also made to determine the compressive strength. The compressive strength for the concretes with a coarse aggregate was determined from $100 \times 100 \times 100$ mm cubes, whereas the strength for those with no coarse aggregates was determined using $50 \times 50 \times 50$ mm cubes. In addition, the flexural tensile strength of concrete without coarse aggregates was determined for some of the mixes thereby testing $40 \times 40 \times 160$ mm prisms according to ASTM C 348.

Several curing processes were used to determine their effects on the resulting compressive strength. Most of the concrete specimens were cured in a moist room at $\sim 30^{\circ}$C for 7 days, followed by exposure to laboratory air ($\sim 30^{\circ}$C) until the time of testing, except for mixes QWF, QOF-1 and QOF-2. QWF specimens were cured in a water bath at $\sim 90^{\circ}$C for 1 day after initial moist curing for 24 h, and the specimens were then exposed to lab air for 27 days. QOF specimens were sealed after casting and cured at $\sim 250^{\circ}$C for 1 day after an initial moist cure of 24 h; the specimens were then exposed to laboratory air for 7 days.

Granite specimens were also tested for their compressive strength and impact resistance for comparison with concrete.

4.2. Materials used

4.2.1. Cement

ASTM Type I normal Portland cement was used for the concrete mixtures with coarse aggregates, while a sulfate-resisting cement with a low calcium aluminate (C_3A) content was used for mixtures with no coarse aggregate and low w/cm. The purpose of using the sulpahte-resisting cement was to reduce the adsorption of high-range water-reducing admixture by the C_3A.

4.2.2. Silica fume

Dry undensified silica fume was used for most of the concrete mixtures. The silica fume had a SiO_2 content of 92% and specific surface area of $\sim 20\,m^2/g$.

4.2.3. Water-reducing admixtures

A retarding admixture[1] was used for concrete mixes NC90 and NC120, and a polycarboxylate-based superplasticizer[2] was used for the concrete mixes with a compressive strength of more than 120 MPa. The former had a solid content of 38%, whereas the latter had a solid content of 23.5%.

[1] W.R. Grace DARATARD 88.

[2] W.R. Grace ADVA 105.

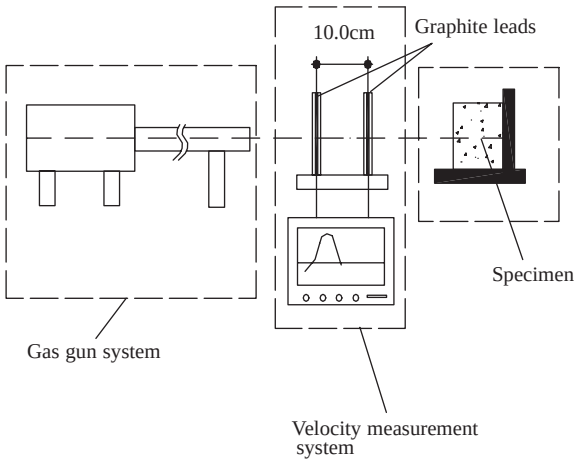

Fig. 1. Schematic graph of the impact test set-up.

4.2.4. Coarse aggregate

Crushed granite with maximum nominal sizes of 20 and 10 mm were used to make concrete of different strengths.

4.2.5. Fine aggregate

Natural sand was used for the concrete mixtures NC40 and NC120. However, for higher strength concrete, quartz sand with a maximum size of 1.18 mm was used. For the quartz sand, three size fractions (0.6–1.18 mm, 300–600 and 150–300 μm) were combined to achieve good grading and to minimize void content. All the aggregates used were in an air-dry condition with a total moisture content of less than 0.1%.

4.2.6. Fibers

Straight steel fibers[3] with a length of 13 mm and a diameter of $\sim$0.2 mm were used for some concrete mixtures. The aspect ratio of the fiber was 65.

4.3. Granite specimens

Granite specimens were cut to the same size as the concrete specimens. The compressive strength of the specimens was about 185.0 MPa, determined from three $50 \times 50 \times 50$ mm cubes.

4.4. Testing and evaluation of impact resistance

The experimental arrangement for projectile impact tests is shown in Fig. 1. A gas gun with a 12.7 mm bore was used. The maximum attainable projectile impact velocity was

[3] BEKAERT ONESTEEL FIBRE DRAMIX OL 13/.20.

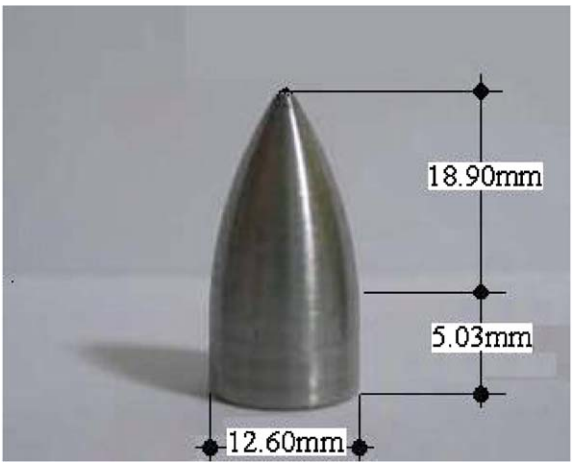

Fig. 2. Projectile.

largely dependent on its mass. In this investigation, ogive-nosed projectiles with a caliber radius head (CRH) of 2.5 and a diameter of 12.6 mm (Fig. 2) were used. The length of the projectile shaft was such that the projectile weighed approximately 15 g. They were propelled by compressed helium at a pressure of about 150 bar to achieve impact velocities of ~620–700 m/s. The projectiles were fabricated from ASSAB grade 8407 supreme tool steel and hardened to 50 Rockwell hardness constant (RHC). After each test, the projectile was examined visually and no damage was observed. However, to ensure consistency in testing, a new projectile was used for each test.

Each test specimen was placed in a containment jig and aligned such that the projectile would hit the center of the specimen. Due to the small size of the projectile, the extent of damage caused by the impact, defined by the penetration depth and crater diameter, depended on whether the projectile struck the coarse aggregate or mortar. Therefore, in most cases, three specimens were used in the testing of each concrete mixture and the average of the results obtained was calculated. To prevent movement of the specimen during impact, two aluminum blocks were placed against the distal face of the specimen.

Impact velocity was measured using a pair of graphite rods placed sequentially in the trajectory of the projectile just before it struck the specimen. The graphite rods formed part of two electrical circuits that were connected to an oscilloscope. Sequential breakage of the rods by the projectile generated voltage changes that were recorded. By relating the time interval between the voltage changes and the distance between the rods, the impact velocity of the projectile could be calculated.

The magnitude of the impact damage induced in the concrete specimens was evaluated from the average crater diameter, maximum penetration depth and degree of crack propagation in the specimen. The average crater diameter was determined by taking the average of four measurements, as shown in Fig. 3. Penetration depth was determined by measuring the distance from the impact surface to the deepest point in the crater. The degree of crack propagation was based on qualitative observation.

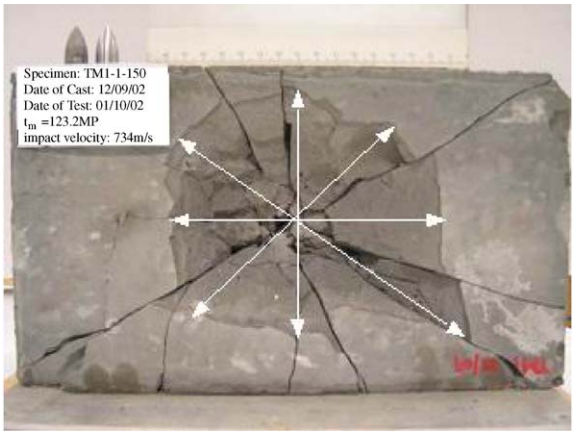

Fig. 3. Determination of crater diameter.

5. Results and discussion

Tables 2–4 summarize the impact test results for 11 concrete mixtures with compressive strengths ranging from about 45 to 235 MPa. The results for granite specimens are also included for comparison. The projectile impact velocity ranged from ~620 to 700 m/s; this difference was expected to affect the degree of damage. Specimens of fiber-reinforced concrete mix NCF90 were subjected to projectile impact at velocities ranging from ~250 to 650 m/s. The results are shown in Fig. 4. The penetration depth increases almost linearly with impact velocity in that range. However, the crater diameter appeared relatively unaffected by impact velocity. Hence, the penetration depth was normalized by dividing it by the impact velocity.

5.1. Effect of compressive strength

Fig. 5 shows experimental results for penetration depth and a comparison with values calculated using formulae recommended by the US Army Corps Engineers (ACE) and National Defense Research Committee (NDRC) [12]:

US Army Corps of Engineers Formula:

$$\frac{P_d}{d} = \frac{3.5 \times 10^{-4} M V_I^{1.5}}{(f_c')^{0.5}\, d^{2.785}} + 0.5.$$

NDRC Formula:

$$G = \left(\frac{P_d}{2d}\right)^2 \quad \text{for} \quad \frac{P_d}{d} < 2.0$$

$$G = \frac{P_d}{d} - 1 \quad \text{for} \quad \frac{P_d}{d} > 2.0,$$

Table 2
Effect of compressive strength and flexural tensile strength on penetration depth and crater diameter for impact on plain concrete (curing temperature = ~30°C)

Specimen designation	w/cm	Type of aggregate/ max size	Ave. compressive strength (MPa)	Std. dev.	Ave. flexural tensile strength (MPa)	Std. dev.	Impact velocity (m/s)	Crater diameter (mm)	Ave.	Std. dev.	Penetration depth (mm)	Normalized penetration depth ($\times 10^3$ mm/m/s)	Ave.	Std. dev.
NC40-1	0.55	Granite/20 mm	45.5	1.2	—	—	668.5	157.5	158.3	3.8	48.0	71.8	71.1	1.2
NC40-2							675.6	155.0			48.5	71.8		
NC40-3							667.7	162.5			46.5	69.6		
NC60-1	0.45	Granite/20 mm	58.3	1.5	5.1	1.1	694.4	149.0	135.9	17.1	46.0	66.2	62.2	4.4
NC60-2							684.9	151.0			45.0	65.7		
NC60-3							657.9	128.0			39.0	59.3		
NC60-4							657.9	115.5			38.0	57.8		
NC90-1	0.31	Granite/10 mm	87.8	1.4	—	—	675.5	133.0	129.3	17.8	41.0	60.7	59.5	1.8
NC90-2							670.7	110.0			38.5	57.4		
NC90-3							679.3	145.0			41.0	60.4		
NC120-1	0.27	Granite/10 mm	112.5	0.9	—	—	677.5	108.0	112.7	4.04	31.0	45.8	44.4	1.7
NC120-2							670.6	115.0			28.5	42.5		
NC120-3							678.2	115.0			30.5	45.0		
CM-150-2	0.23	Quartz/1.18 mm	150.9	1.7	13.0	1.5	646.6	125.0	132.8	31.5	31.0	47.9	50.3	5.0
CM-150-3							634.2	178.0			36.5	57.6		
CM-150-4							675.7	105.0			31.5	46.6		
CM-150-5							684.9	123.0			33.5	48.9		
Granite-1	—	—	185.0	0.5	—	—	640.0	30.0	33.7	4.4	10.0	15.6	17.4	3.3
Granite-2							660.5	38.5			14.0	21.2		
Granite-3							645.5	32.5			10.0	15.5		

Table 3
Effect of steel fibers on penetration depth and crater diameter (curing temperature = ~30°C)

Specimen designation	w/cm	Steel fiber content (%)	Type of aggregate/ max size	Ave. compressive strength (MPa)	Std. dev.	Ave. flexural tensile strength (MPa)	Std. dev.	Impact velocity (m/s)	Crater diameter (mm)	Ave.	Std. dev.	Penetration depth (mm)	Normalized penetration depth ($\times 10^3$ mm/m/s)	Ave.	Std. dev.
NC90-1	0.31	—	Granite/10 mm	87.8	1.4	—	—	675.5	133.0	129.3	17.8	41.0	60.7	59.5	1.8
NC90-2		—						670.7	110.0			38.5	57.4		
NC90-3		—						679.3	145.0			41.0	60.4		
NCF90-1		1.5		93.5	1.2	—	—	665.0	82.5	87.8	—	38.0	57.1	57.1	—
NCF90-2		1.5						640.5	93.0			36.5	57.0		
NC120-1	0.27	—	Granite/10 mm	112.5	0.9	—	—	677.5	108.0	112.7	4.0	31.0	45.8	44.4	1.7
NC120-2		—						670.6	115.0			28.5	42.5		
NC120-3		—						678.2	115.0			30.5	45.0		
NCF120-1		1.5		115.0	1.2	—	—	678.0	70.0	63.5	—	33.5	49.4	46.2	—
NCF120-2		1.5						650.0	57.0			28.0	43.1		
CM-150-2	0.23	—	Quartz/1.18 mm	150.9	1.7	13.0	1.5	646.6	125.0	132.8	31.5	31.0	47.9	50.3	5.0
CM-150-3		—						634.2	178.0			36.5	57.6		
CM-150-4		—						675.7	105.0			31.5	46.6		
CM-150-5		—						684.9	123.0			33.5	48.9		
QFF-1		1.5		187.2	1.5	31.5	1.5	644.3	85.0	75.8	8.8	39.0	60.5	53.5	8.6
QFF-2		1.5						694.4	67.5			30.5	43.9		
QFF-3		1.5						704.2	75.0			39.5	56.1		

Table 4
Effect of curing temperature on penetration depth and crater diameter in concrete (steel fibers 1.5% by volume of concrete, quartz aggregate/maximum size 1.18 mm)

Specimen designation	w/cm	Curing temperature (°C)	Ave. compressive strength (MPa)	Std. dev.	Ave. flexural tensile strength (MPa)	Std. dev.	Impact velocity (m/s)	Crater diameter (mm)	Ave.	Std. dev.	Penetration depth (mm)	Normalized penetration depth ($\times 10^3$ mm/m/s)	Ave.	Std. dev.
QFF-30-1	0.23	~30	187.2	1.5	31.5	1.5	644.3	85.0	75.8	8.8	39.0	60.5	53.5	8.6
QFF-30-2							694.4	67.5			30.5	43.9		
QFF-30-3							704.2	75.0			39.5	56.1		
QWF-90-1	0.23	90	183.6	1.7	32.6	1.6	637.6	85.0	84.8	2.8	35.5	55.7	52.0	7.7
QWF-90-2							621.3	82.0			35.5	57.1		
QWF-90-3							694.4	87.5			30.0	43.2		
QOF-1-1	0.23	250	203.5	1.5	32.8	1.7	653.0	87.0	84.0	3.6	35.0	53.6	51.0	2.3
QOF-1-2							644.5	85.1			31.0	48.1		
QOF-1-3							625.0	80.0			32.0	51.2		
QOF-2-1	0.18	250	237.0	1.6	33.0	1.7	620.0	81.0	83.5	2.2	28.5	46.0	46.0	1.1
QOF-2-2							647.5	85.0			30.5	47.1		
QOF-2-3							636.0	84.5			28.5	44.8		

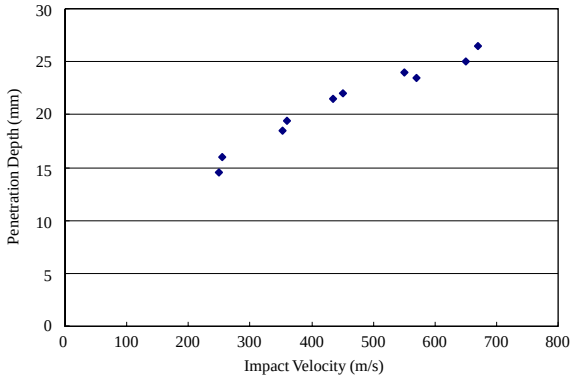

Fig. 4. Effect of impact velocity on penetration depth for concrete NCF90.

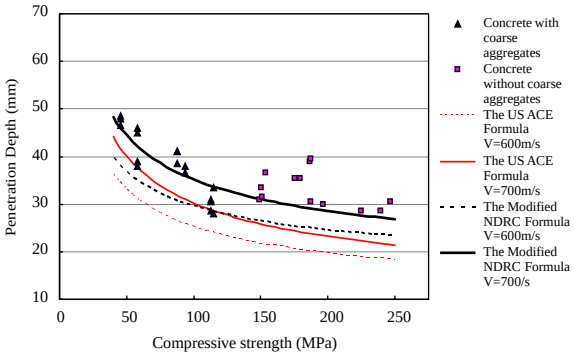

Fig. 5. Effect of compressive strength on penetration depth in concrete.

where

$$G = \frac{3.8 \times 10^{-5} N M V_{\mathrm{I}}^{1.8}}{f_{\mathrm{c}}'^{0.5} d^{2.8}}$$

and P_{d} is the penetration depth (m), d is the projectile diameter (m), M is the projectile mass (kg), f_{c}' is the ultimate compressive strength of concrete (Pa), V_{I} is the impact velocity (m/s), N is the projectile shape factor; 1.14 for a sharp projectile.

The test results indicate that in general, penetration depth decreases with an increase in the compressive strength. However, above a certain level, further increase in the compressive strength does not have a significant effect on penetration depth. A comparison of the experimental results with values calculated using the ACE and NDRC formulae shows that the ACE formulae seem to underestimate penetration depth, whereas the NDRC formula provides reasonable estimates for concrete with a compressive strength up to about 115 MPa; beyond that, the NDRC formula also underestimates the penetration depth. These empirical formulae were developed for ordinary concrete and impact velocities less than $\sim$310 m/s [12]. Both the ACE and NDRC formulae suggest that penetration depth is related to the square root of the compressive strength. According

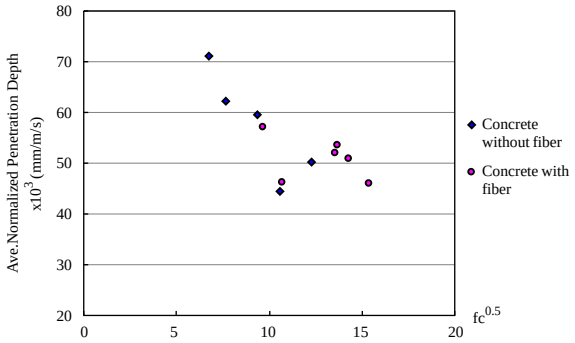

Fig. 6. Relationship between average normalized penetration depth and the square root of the compressive strength of concrete.

to the relationship shown in Fig. 6, it seems that the normalized penetration depth reduced with the square root of compressive strength to a certain level, beyond which it does not reduce further.

Upon impact by a projectile, it is possible that high compressive stresses are exerted by the projectile tip on the concrete specimens, whereas high shear stresses would be induced at the circumference in the specimens. Therefore, a higher compressive strength would impede penetration by the projectile, while a higher tensile strength may reduce the crater size by inhibiting fracture.

Further analysis of the test data indicated that use of coarse aggregate and fibers had significant effects on impact resistance. These are discussed in the following sections.

5.2. *Effect of the coarse granite aggregate*

Table 2 shows the impact resistance of plain concrete in terms of penetration depth and crater size, in relation to granite specimens. For plain concrete with a compressive strength of 112.5 MPa (w/cm = 0.27) the average penetration depth and crater diameter were, respectively, 40% and 60% lower than that for the concrete with a compressive strength of 45 MPa (w/cm = 0.55). Further reduction of the w/cm ratio to 0.23 and elimination of the coarse aggregate increased the compressive strength to 150 MPa (Mix CM), but resulted in an increased penetration depth and crater diameter, compared to concrete with a compressive strength of 115 MPa. This indicates that although the reduction of w/cm and maximum aggregate size reduced heterogeneity and increased the compressive strength of the concrete, it did not improve the impact resistance. The presence of coarse aggregate appears to be beneficial with respect to impact resistance and hinders crack propagation.

Fig. 7 shows the damage induced on the front face of concrete specimens with compressive strengths ranging from 45 to 150 MPa, together with a granite specimen for comparison. To illustrate the impact damage more clearly, only the damaged areas of various specimens are shown, rather than the entire front face. Brittle failure was observed for all plain concrete specimens.

For concrete with coarse aggregates, the crater appears to be limited to the front half of the specimens regardless of the concrete strength. For concrete with a compressive strength of 45 MPa (NC40), large cracks extend through the height of the specimen to the distal face for all the three

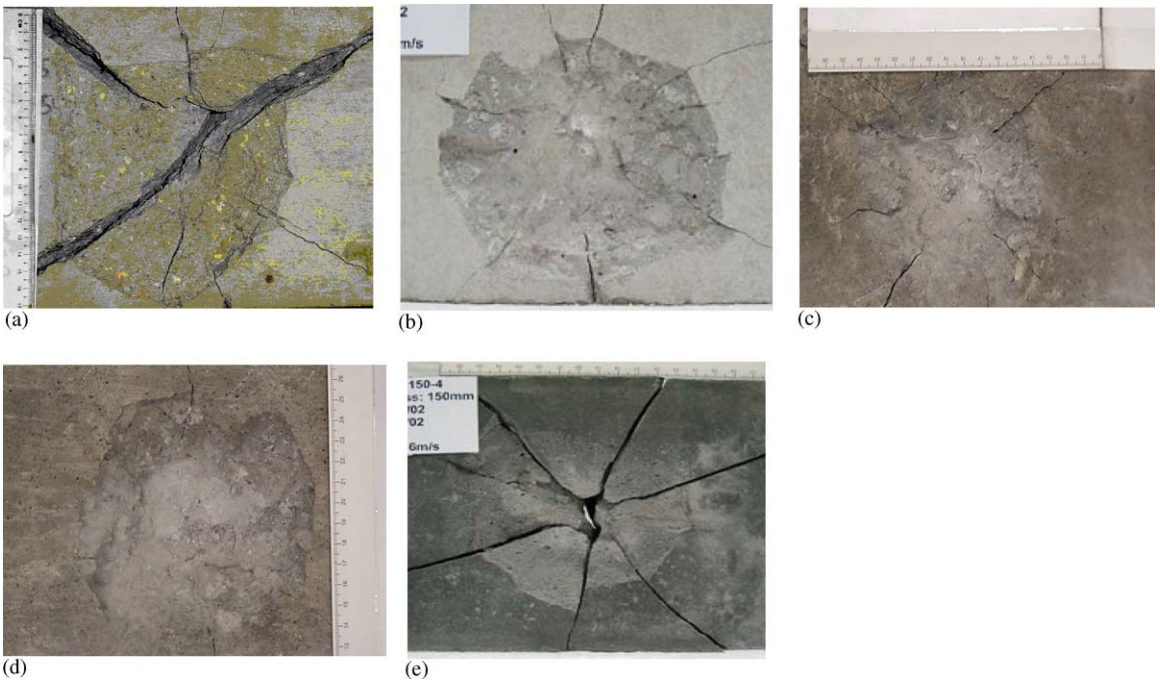

Fig. 7. Front face damage of the plain concrete with compressive strength from 45 to 150 MPa and that of the rock specimen: (a) NC40, (b) NC60, (c) NC90, (d) NC 120, and (e) CM150.

specimens tested and the specimens split into several pieces. For concrete with a compressive strength of 60 MPa (NC60), no large crack was found on the distal face of all three specimens, except for a hairline crack extending partially down the height of the specimen. For concrete with compressive strengths of 90 and 115 MPa (NC90 and NC120), there was no visible crack on the distal face of any of the specimens. For NC90 specimens, there were less prominent cracks radiating from the crater on the impact face, compared to those on NC60 specimens. For concrete with a compressive strength of 115 MPa (NC120), only limited hairline cracks were observed to radiate from the crater region on the impact face.

For concrete with a compressive strength of 150 MPa (CM) (no coarse aggregate), most of the specimens exhibited brittle failure and cracks extended right through the specimens to the distal face, splitting the specimens into pieces.

It should be noted that under impact loading, the rapid increase in stress in the specimens drive a large number of microcracks into rapid extension. Thus, these cracks might be forced to propagate through the coarse aggregates rather than around them [13,14]. Since granite is formed from the solidification of molten rock matter either above or below the earth's surface, aggregate derived from granite is generally stronger than the cement paste and the interfacial zone between them (as highlighted earlier). Crack propagation is thus reduced when coarse aggregate is present. A comparison between the failure modes in concrete with and without coarse aggregate confirms the benefit of including coarse aggregates, which act as barriers to crack propagation.

Observations relating to the granite specimens, which are similar to the coarse aggregate used in the concrete, are summarized in Table 2. It is obvious that the penetration depth and crater diameter are much smaller than those in ordinary and high strength concrete. For granite specimens, the penetration depth and crater diameter were about three times smaller than those in ordinary concrete with a strength of 45 MPa, and more than 1.5 times lower than those in high strength concrete with a compressive strength of 115 MPa.

These results indicate that increasing the coarse aggregate content and reducing the w/c improves impact resistance, as long as workability of the concrete is satisfied.

5.3. Effect of fibers

The effectiveness of incorporating fibers in terms of enhancing the mechanical properties of brittle cementitious composites arises from load transfer from the brittle matrix to the fibers and the bridging effect of the fibers across cracks propagating in the matrix. From the data in Table 3, it appears that the presence of 1.5% steel fibers by volume resulted in reduced crater diameters, but did not affect penetration depth substantially. Crater diameters in fiber-reinforced concrete were, respectively, 40–80% smaller than those in plain concrete; this probably comes from improvement in the flexural tensile strength.

Comparing the nature and severity of impact damage with that induced in plain concrete, the incorporation of 1.5% steel fibers reduces crack propagation beyond the crater region, so that damage becomes confined to a localized area. For corresponding plain concrete without fibers, the failure induced appeared brittle and cracks extended beyond the crater region and in some cases, split the specimens into pieces.

It was found that cracking generally reduced with an increase in the strength of fiber-reinforced concrete from 90 to 115 MPa. Further increases in strength to 185 MPa actually increased crater size and penetration depth. This is probably related to the effect of the coarse aggregate which is generally stronger than the cement paste, as discussed earlier.

Since the cost of concrete with compressive strengths of $\sim$115 MPa is much lower than their high-strength counterparts (185 MPa), the former is more cost-effective.

5.4. Effect of curing temperature

Since granite has better impact resistance than high-strength concrete, the impact resistance of the concrete may be enhanced by improving the cement paste. Generally, the strength of the cement paste may be improved either by reducing the w/cm ratio and porosity, or by changing the nature of the hydration reaction products.

From laboratory tests, the w/cm can be reduced to $\sim$0.20 without significantly affecting workability. However, beyond this, workability would be reduced to the extent that the concrete may have a higher porosity and lower strength because of difficulty in consolidation. Therefore, the effect of high temperature curing was studied to determine if a change in the nature of the hydration reaction products would affect concrete strength and impact resistance. According to Richard and Cheyrezy [8], curing cement paste at 250°C results in the formation of crystalline calcium silicate hydrate xonolite C_6S_6H, which differs from generally amorphous calcium silicate hydrates formed in cement pastes cured at room temperature. They attributed the improved

strength of the cement paste cured at 250°C to the formation of crystalline calcium silicate hydrates.

The effect of curing temperature on the strength and impact resistance of concrete with a w/cm of 0.23 is presented in Table 4. An increase in the curing temperature from ~30°C to 90°C did not affect the strength and penetration depth significantly. However, a further increase in curing temperature to 250°C increased the compressive strength by ~10%, but had no effect on the flexural tensile strength and impact resistance. No visible cracking outside the crater region was observed for specimens cured at ~30°C. However, short hair-line cracks radiating from the crater were observed in two of the three specimens cured in a 90°C water bath, and in one of the three specimens cured at 250°C.

For the specimens cured at 250°C, a further reduction in the w/cm ratio from 0.23 to 0.18 increased the compressive strength by about 15% and reduced penetration depth by 10%, but did not affect the crater diameter significantly. No visible cracks outside the crater region were observed.

6. Conclusions

The present study on projectile impact resistance of concrete with compressive strengths ranging from 45 to 235 MPa against penetration by a 15 g ogive-nosed projectile impinging at ~620–700 m/s indicates the following:

1. The penetration depth and crater diameter induced in the concrete targets reduces with a decrease in the water-to-cementitious material ratio (w/cm) and an increase in the compressive strength of the concrete. For plain concrete with a compressive strength of 115 MPa, the penetration depth and crater diameter were respectively, 40% and 60%, lower than those in concrete with a compressive strength of 45 MPa. However, these trends were not linear. A further increase in the compressive strength requires a reduction in the w/cm ratio and the elimination of coarse aggregate. However, doing this did not result in a reduction in penetration depth and crater diameter. The incorporation of coarse aggregate improves impact resistance in terms of reducing penetration depth, crater diameter and crack propagation.
2. The granite specimens exhibited better impact resistance compared with high-strength concrete. The penetration depth and crater diameter in granite specimens were three times smaller than that in ordinary concrete with a strength of 45 MPa; even when compared with high strength concrete with a compressive strength of 115 MPa, these quantities were smaller by more than 1.5 times.
3. The incorporation of steel fibers in concrete reduced the crater diameter and crack propagation, but did not have a significant effect on penetration depth.
4. An increase in the curing temperature from 30°C to 250°C did not influence the impact resistance of concrete significantly.
5. Consideration of the experimental findings in the light of fabrication costs indicate that high-strength fiber-reinforced concrete with a compressive strength of ~100 MPa is an efficient material for protection against projectile impact.

Acknowledgements

The authors would like to acknowledge the Defence Science and Technology Agency of Singapore for funding this project. Also, the contributions of Mr. Roy C.W. Ong towards the development of high-strength concrete are gratefully recognized.

References

[1] Clifton JR. Penetration resistance of concrete—a review. Special Publication, National Bureau of Standards, Washington, DC, 1982. p. 480–5.
[2] Hanchak SJ, Forrestal MJ, Young ER, Ehrgott JQ. Perforation of concrete slabs with 48 MPa (7 ksi) and 140 MPa (20 ksi) unconfined compressive strengths. Int J Impact Eng 1992;12(1):1–7.
[3] Dancygier AN, Yankelevsky DZ. High strength concrete response to hard projectile impact. Int J Impact Eng 1996;18(6):583–99.
[4] Anderson WF, Watson AJ, Armstrong PJ. Fiber reinforced concretes for the protection of structures against high velocity impact. In: Morton J, editor. Proceedings of the International Conference on Structural Impact and Crashworthiness. London: Imperial College; 1984. p. 687–95.
[5] Anderson WF, Watson AJ, Kaminskyj AE. The resistance of SIFCON to high velocity impact. Bulson PS, editor. Proceedings of the Second International Conference on Structures Under Shock and Impact, Portsmouth, UK. 1992. p. 89–98.
[6] O'Neil EF, Neeley BD, Cargile JD. Tensile properties of very-high-strength concrete for penetration-resistant structures. Shock Vib 1999;6:237–45.
[7] Langberg H, Markeset G. High performance concrete-penetration resistance and material development. Proceedings of the Ninth International Symposium on Interaction of the Effects of Munitions with Structures, Berlin-Strausberg, 1999. p. 933–41.
[8] Richard P, Cheyrezy M. Composition of reactive powder concretes. Cem Concr Res 1995;25(7):1501–11.
[9] Lankard DR. Slurry infiltrated fiber concrete (SIFCON) properties and applications. Proceedings of the Material Research Society, Fall Meeting, vol. 42, Boston, USA, 1984. p. 277–86.
[10] Hackman LE, Farrell MB, Dunham OO. Slurry infiltrated mat concrete (SIMCON). Concr Int 1992;14(12):53–6.
[11] Hauser S, Wörner JD. DUCON, a durable overlay. Proceedings of the Third International Workshop on High Performance Fiber Reinforced Cement, 1999. p. 603–15.
[12] Martin SQ. Modeling of local impact effects on plain and reinforced concrete. ACI Struct J 1994;91(2):178–87.
[13] Zielinski AJ. Fracture of concrete under impact loading. Morton J, editor. Proceedings of the International Conference on Structural Impact and Crashworthiness. London: Imperial College; 1984. p. 654–65.
[14] Bentur A, Mindess S. The effect of concrete strength on crack patterns. Cem Conc Res 1986;16:59–66.